ELSEVIER

Catalysis Today 54 (1999) 107–118

CATALYSIS TODAY

www.elsevier.com/locate/cattod

Perovskites as polyvalent catalysts for total destruction of C_1, C_2 and aromatic chlorinated volatile organic compounds

G. Sinquin *, J.P. Hindermann, C. Petit, A. Kiennemann

LERCSI-ECPM-UMR ULP-CNRS 7515, 25, rue Becquerel, 67087 Strasbourg Cédex 2, France

Abstract

Perovskites ABO_3 (A: La, B = Co, Mn) have shown to be effective and polyvalent in catalytic total oxidation of chlorinated volatile organic compounds such as chlorinated methanes, and chlorinated saturated and unsaturated C_2 hydrocarbons and chlorobenzene. Perovskites prepared by a sol–gel like method are characterised before and after catalytic test. The difference in behavior of the manganese and cobalt containing catalysts is discussed and attributed to an oxygen overstoichiometry in the manganese catalyst. Differences have also been observed in reaction mechanisms depending on the reacting chlorinated molecule. ©1999 Elsevier Science B.V. All rights reserved.

Keywords: Chlorinated VOC; Catalytic total oxidation; Perovskites; Reaction mechanism

1. Introduction

Due to their inertness and their widespread application in industry, halogenated and more specially chlorinated, volatile organic compounds play an important role in air and water pollution. Thus according to Siddebottom et al. [1], about 1.5 millions tonnes of chlorinated compounds are released each year into atmosphere in the world. Further, incineration of municipal wastes is also a source of polychlorinated dioxins and dibenzo-furans which are highly toxic. Chlorinated compounds are not only harmful directly for public health but their long lifetimes results in accumulation in the environment and the depletion of the stratospheric ozone layer. Thus, the abatement of chlorinated volatile organic compounds (CVOCs) emission is highly important.

Today the most commonly used process for elimination of CVOCs is the thermal incineration, which requires temperatures near 1000°C to achieve complete combustion. These high temperatures generate expensive costs because of corrosion. Nitrogen oxides (NO_x) are formed, dioxins and dibenzofurans [2] may be produced.

Catalytic combustion has the advantage to be carried out at relatively low temperatures (<500°C) and is, therefore, a highly energy efficient process compared to thermal incineration especially in the case of low concentrations. A catalytic process has a good potential for high selectivity to the formation of harmless reaction products, leading thus to a complete destruction of all halocarbons including the toxic by-products.

Two main types of catalysts are reported in the literature [3]: supported noble metal and metal oxides or mixtures of metal oxides. The noble metals (Pt and/or

---

* Corresponding author. Tel.: +33-3-88-13-69-73; fax: +33-3-88-13-69-75
E-mail address: kiennemann@chimie.u-strasbg.fr (G. Sinquin)

PII: S0920-5861(99)00173-X

Pd) deposited on various supports like SiO_2, TiO_2 and more often Al_2O_3 have been extensively studied [4–10]. However, it seems that these catalysts are more or less deactivated. Reports on deactivation of these catalysts are controversial, and many of the authors have not considered the ageing. Windawi and Zhang [5] and Friedel et al [11] claim that after a slight initial deactivation, the activity is stabilized whereas numerous authors point to deactivation at low temperatures ($T < 350$–400°C) [12–14]. HCl is thought to be responsible for the deactivation and it seems that small metal crystallites deactivate more easily [12]. Therefore, the crystallite size being in general linked to the amount of the metal, concentrations higher than 0.3% of platinum are necessary to produce a stable catalyst which makes them expensive.

Among the metal oxide catalysts, chromium oxide supported on Al_2O_3, or not, seems to be the most effective one [15–18].

A fast deactivation was observed in the catalytic oxidation in dry air of various chlorinated compounds on a 12.5% Cr_2O_3/Al_2O_3 catalyst and a red deposit, formed at the exit of the reactor, suggested the formation of the volatile red chromium oxychloride (CrO_2Cl_2). [19]. The same deactivation resulted from the oxidation of perchloroethylene using a Cr_2O_3/Al_2O_3 catalyst, the conversion drops from 98 to 53% over 17 h and was correlated with a drop of chromium content from 12.5 to 7.5%. The addition of water slowed the deactivation but did not eliminate it [20]. The reduced deactivation rate upon water addition is probably due to the reverse Deacon reaction:

$$H_2O + Cl_2 \leftrightarrows 2HCl + \tfrac{1}{2}O_2$$

which removes Cl_2 from the product gas flow. More details about deactivation of chromia containing catalysts are given in [21].

The starting idea of the present work was to stabilize the active metal oxides in incorporating them into a well defined structure. Mixed oxide systems of well defined ABO_3 structure (perovskites) were originally chosen because of their well known performances in total oxidation of hydrocarbons and/or CO as reviewed in [22]. The present work was started in 1994 as part of a contract with the European Community. Since a few papers on the subject appeared in literature [23–26], but to our knowledge, no complete study on the activity, selectivity and stability of the catalyst has been published. Preliminary results in our laboratory have shown that manganese and cobalt oxides are good potential candidates and the $LaMnO_{3+\delta}$ and $LaCoO_3$ perovskites have been selected to probe the catalytic total oxidation of chloromethane, chloroethanes and ethenes, and chlorobenzene.

2. Experimental

2.1. Preparation of catalysts

The perovskites containing Mn or Co, $LaMnO_{3+\delta}$ and $LaCoO_3$ have been prepared by the sol–gel like method with propionic acid as solvent [27]. Hydrated Mn or Co nitrates have been used as precursors. Lanthanum is introduced as an oxide after calcination at high temperature (800°C) in order to decompose the hydroxide. La_2O_3 is dissolved slowly in hot propionic acid to produce the corresponding propionate [28]. The transition metal salt is dissolved separately depending on the desired perovskite. After obtention of two limpid solutions, they are mixed and stirred for 1 h under reflux. The resulting solution is evaporated at atmospheric pressure to eliminate most of the solvent until formation of the resin. Nitrous vapors are then evacuated at reduced pressure. By cooling the resin hardens readily and must be recuperated by crushing in liquid nitrogen.

The resulting solid was calcined at various temperatures for 4 h after a temperature increase from room temperature to the chosen calcination temperature with a slope of 3°C min^{-1}. The obtained samples were analyzed by XRD and the BET surface areas have been measured. An example is given for the $LaCoO_3$ perovskite in Table 1. An optimized calcination temperature was chosen at which no other crystalline phases were observed than the perovskite structure and a reasonable surface area was still obtained.

The calcination temperature for the various perovskites and the corresponding surface areas are summarized in Table 2.

Further, the catalysts have been characterized by XRD, FTIR, XPS and elemental analyses. More details about preparation and characterization are given in [29]. As a summary the Co perovskite has the conventional $LaCoO_3$ structure whereas the Mn perovskite is overstoichiometric in oxygen ($LaMnO_{3.15}$).

Table 1
Influence of calcination temperature on BET surface area and crystallinity of $LaCoO_3$

Calcination		BET surface area ($m^2\,g^{-1}$)	Crystalline state
Temperature (°C)	Duration (h)		
600	16	26.7	Poor crystallinity Presence of La_2O_3 and Co_3O_4 phases
700	8	8.9	Good crystallinity No other phases observed
800	8	2.1	Good crystallinity No other phases observed

Table 2
Calcination temperature, BET surface area of the used samples and catalytic activity for CH_2Cl_2 oxidation represented as specific rate at 340°C and T_{50}, T_{90} values. T_{50} and T_{90} are, respectively, temperatures at which 50 and 90% of CH_2Cl_2 are converted

Catalysts	Calcination temperature (°C)	BET surface area ($m^2\,g^{-1}$)		T_{50} (°C)	T_{90} (°C)	Specific rate at 340°C (μmol h^{-1} m^2)
		Before test	After test with CH_2Cl_2			
$LaCrO_3$	600	3.3	3.7	500	–	1.05
$LaMnO_{3+\delta}$	750	17.1	12.4	355	440	0.77
$LaFeO_3$	650	8.8	5.7	380	445	1.11
$LaCoO_3$	700	9.8	12.7	320	420	2.36
$GdCoO_3$	800	3.5	3.3	380	480	3.52
$SnCoO_3$	800	3.7	8.1	370	470	3.76
$La_{0.6}Sr_{0.4}CoO_3$	750	8.8	8.5	415	495	0.85

2.2. Testing device and operation conditions

A more complete description of the testing device is given in [29]. It will only be recalled briefly here. The various inlet gas flows (O_2, $CH_{4-x}Cl_x$ are regulated by mass flowmeters (BROOKS 5850). Water is introduced by passing helium through a bubbler. The glass reactor has an internal diameter of 5 mm and contains 0.5 g of sieved catalyst with particle sizes in between 0.125 and 0.250 mm. The operating conditions are: CVOCs concentration in order to produce 2000 ppm of HCl at total conversion and 100% HCl selectivity (e.g. 1000 ppm CH_2Cl_2 or 500 ppm of CCl_4 in standard conditions). An overall flow of 6 l h^{-1} g cat^{-1} is maintained constant by adjusting the helium flows by two mass flowmeters (BROOKS), one of the gas flows passing through a bubbler containing water. The chlorinated hydrocarbons (either the parent molecules and the resulting by-products) are analyzed by gas chromatography with a chlorinated compound specific column (column RTX 502.2 from Restek, G.C. VARIAN 3400 CX). CO_2 and CO have been quantified by a self-made device. A conventional injector is used to introduce the reference CO_2-He mixture (1000 ppm CO_2). A 3-way sampling valve sends the outlet gases either to the GC for analysis of the chlorinated hydrocarbon or into an Intersmat IGC 120 GG apparatus (to separate CO and CO_2). These two gases are transformed to methane in a methanizer with a Raney nickel catalyst. The resulting methane is quantified on a Varian 3400 CX G.C. apparatus with a FID detector.

Prior to the test the catalyst is preheated under O_2 in presence of water up to 350°C. At 350°C the chlorinated molecule is injected and the outlet gases are monitored by on-line chromatographs and mass spectrometer (QTMD mass spectrometer from Fison Instruments). Steady state is reached after about 3 h, and the system is maintained at 350°C during one night prior to the test.

2.3. Characterization of catalyst

BET surface areas have been measured using a SA 3100 Coulter Sorptometer at 77 K. XPS spectra were obtained with a Vacuum Generator (VG) ESCA3 device at 10^{-8} Torr using Al Kα radiation

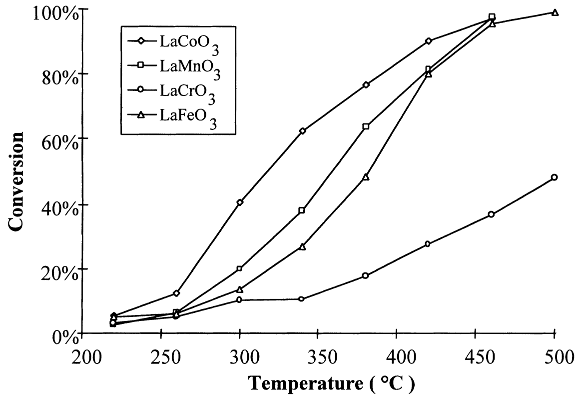

Fig. 1. Conversion curves of 140 ppm of CH_2Cl_2 on $LaBO_3$ perovskites (3.3% O_2, 1.3% H_2O in He).

($h\nu = 1486.6$ eV). The sample were out gassed at room temperature prior to analysis. The decomposition of the spectra was performed by the software of Romeo et al. [30,31]. The spectra have been calibrated relatively to the $C1s_{1/2}$ binding energy of contamination carbon at 284.6 eV.

XRD experiments were performed at room temperature on a D5000 Siemens diffractometer using the Cu Kα radiation ($\lambda = 0.15406$ nm) operated at 20 mA and 40 kV. The scattering were measured over an angular range of $20° < 2\theta < 85°$ for all sample with a step $\Delta(2\theta)$ of 0.03 and a count time of 2 s per step. The diffractograms have been indexed by comparison with the JCPDS files (Joint Committe on Powder Diffraction Standards).

Infrared spectra were recorded on a FTIR Nicolet 5DXC apparatus. The perovskite (3%) were mixed with KBr and pressed to form a disc of about 100 mg and 1 cm^2 with a 4 cm^{-1} resolution.

3. Results and discussion

3.1. Reactivity

Preliminary results obtained with 140 ppm of CH_2Cl_2 have shown that among the tested perovskites $LaMnO_{3+\delta}$ and $LaCoO_3$ gave the best results as can be seen on Figs. 1 and 2.

If the specific surface rates (in μmol h^{-1} m^{-2}) are considered (Table 2) at initial time one can conclude that $GdCoO_3$ and $SmCoO_3$ are potentially good catalysts. However, these catalysts are rapidly deactivated and they could not be obtained with higher surface areas in the present study. $LaCoO_3$ has a good initial specific rate but it is deactivated for CH_2Cl_2 oxidation. Thus, in an aging experiment the initial conversion was adjusted at 99% and drops to 74% after six days on stream. Whereas for $LaMnO_{3+\delta}$, the activity changes only from 99% to 96%. $LaMnO_{3+\delta}$ has the lowest specific activity, however higher surface areas are obtained and the activity per weight of the catalyst is higher.

If the formation of higher chlorinated by-products are considered ($CHCl_3$ and CCl_4), it was observed that $LaMnO_{3+\delta}$ produced only traces amounts and that the performance of $LaMnO_{3+\delta}$ are better than that of $LaCoO_3$. It is known from literature that CH_2Cl_2 is one of the most difficult molecule to be destroyed by catalytic oxidation. The behavior of the perovskite for C_1 molecules have been discussed more thoroughly in [29,32]. It was concluded, by the study of the by-product formation and the influence of water addition to the feed, that the reaction mechanism differed for the three C_1 molecules. The differences in reaction mechanisms could be explained in taking into account the known chemistry of nucleophilic attack of chlorinated compounds in liquid media. The differences of the effect of water in the oxidation of the molecules could be rationalized in terms of solvent assisted proton transfer as the possibility has been evoked by Haw et al. for catalysis on zeolites [33]. The difference of the oxygen dependence of

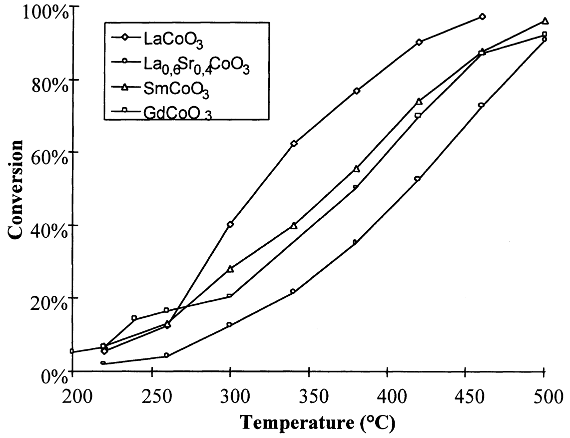

Fig. 2. Conversion curves of 140 ppm of CH_2Cl_2 on $LnCoO_3$ perovskites (3.3% O_2, 1.3% H_2O in He) (Ln = rare earth).

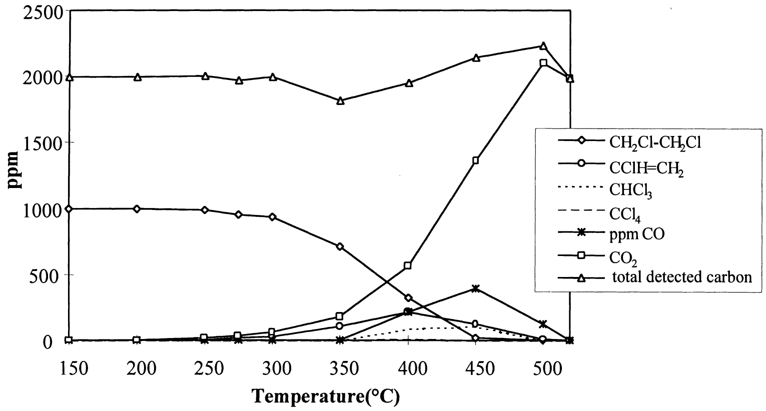

Fig. 3. Oxidation of 1000 ppm of $CH_2Cl–CH_2Cl$ on 0.5 g $LaMnO_{3+\delta}$ (3.3% O_2, 1.3% H_2O in He).

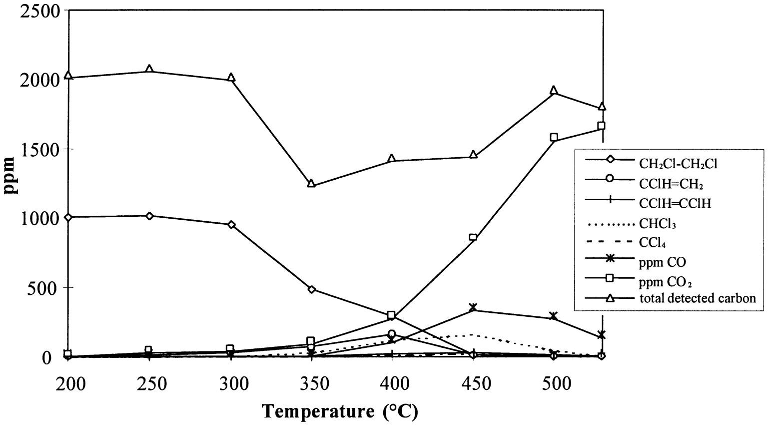

Fig. 4. Oxidation of 1000 ppm of $CH_2Cl–CH_2Cl$ on $LaMnO_{3+\delta}$ (3.3% O_2 in He without water).

CCl_4 reaction compared to CH_2Cl_2 can also be explained by a difference in reaction mechanism if one considers that the CCl_4 reaction is of the S_N1 type with formation of a $^+CCl_3$ carbocation and its reaction with the weak nucleophile water. For CH_2Cl_2 a S_N2 type mechanism would explain the necessity to provide oxygen since the oxygen contained in the end product would originate from the surface which must be reoxidize to be able to destroy another molecule of CH_2Cl_2 [29,32].

The mechanism proposed from CH_2Cl_2 destruction is in agreement with the results of infra-red study on CH_2Cl_2 adsorption on γAl_2O_3 [34].

Given the encouraging results obtained with the chlorinated C_1 molecules the two perovskites have been tested in the catalytic destruction of C_2 hydrocarbons. 1,2-dichloroethane was chosen as a model for chlorinated C_2 saturated hydrocarbons. Mochida et al. [35] have observed during the dehydrochlorination of various chloroethanes, that this reaction is slowest with 1,2-dichloroethane. This compound is thus the most convenient to study the difference of behavior between saturated and unsaturated chlorinated hydrocarbons. The results obtained for the catalytic oxidation of 1,2-dichloroethane on $LaMnO_{3+\delta}$ in presence of water and oxygen are given on Fig. 3. It can be seen that the T_{50} and T_{90} values (temperature at which 50 and 90% conversion of 1,2-dichloroethane are achieved) are 370 and 430°C, respectively.

The main observed by-product is vinyl chloride a result of the dehydrochlorination reaction, together with formation of some CO. Total conversion of all by-products including CO is obtained at about 500°C. In order to study the influence of water the same reaction was performed in the same conditions with a dry feed gas, the result are given in Fig. 4.

If one considers only the rate of disappearance of 1,2-dichloroethane ($T_{50} = 350$ and $T_{90} = 430$°C), one could conclude that water has little, or a slight deactivating, influence (Fig. 5). However, considering the carbon balance it can be seen that a defect of about 40 to 30% is observed between 350 and 450°C, that means that all the by-products of the reaction are not detected.

A possible explanation of the bad carbon balance could be the polymerization of vinylchloride either on the catalytic bed or at the exit of the reactor. The influence of water on the formation of the polymer could be explained in two ways:

1. Water could inhibit the polymerization of the formed vinyl chloride. It is known that in presence of a Lewis acid undergoes an intermolecular dehydrochlorination with conjugated double bond formation [36]. Water could compete for the Lewis acid sites preventing fast polymerization, and vinyl chloride could further be oxidize before polymerization.
2. Water diminishes the rate of vinylchloride formation and hence the probability of polymerization. The retardation effect of water on the dehydrochlorination has been reported by Ballinger et al. [37] for 1,1,1 trichloroethane on alumina. They attributed this to the fact that Lewis acid sites are responsible for the dehydrochlorination. Vinylchloride could be formed through a chloroethylcarbonium ion that loses a proton to form vinyl chloride [38]. The vapour-phase intramolecular dehydrochlorination of dichloroethane is an industrial method of obtaining vinyl chloride, the reaction is effected at 300–400°C on acid catalysts (zinc chloride, iron chloride, alumino-silicates etc.) in these conditions there is little probability of collision of two molecules of dichloroethane on the catalyst surface [36]. That explains why in absence of water at higher temperatures the activity is restored and the carbon balance is again complete.

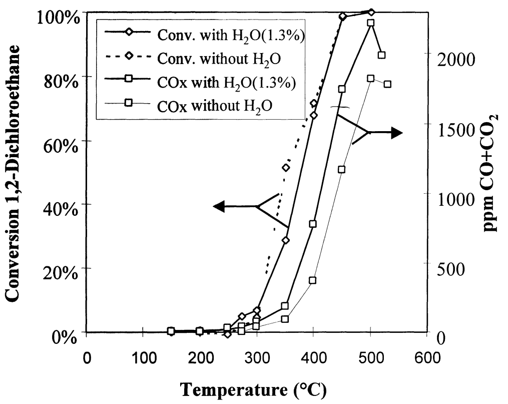

Fig. 5. Oxidation of $CH_2Cl–CH_2Cl$ on $LaMnO_{3+\delta}$. Influence of water addition on the formation of CO_x ($CO+CO_2$).

Imamura et al. [39] have studied the decomposition of 1,2-dichloroethane. They observed that with Y zeolite or aluminosilicate, they had a bad carbon and chlorine balance and they observed the formation of a carbonaceous deposit by ESR. However, this deposit only accounts for 1/10th of the carbon missing in the carbon balance. In fact they reported that an unknown product was observed by gas chromatography. This unknown product might well have been vinylchloride. They observed that on titania/silica catalysts not only the acidic site but also a redox activity is necessary to have a complete decomposition to CO_2 and HCl. The reaction of 1,2-dichloroethane in presence of water and absence of oxygen is shown in Fig. 6.

It can be observed that the formation of vinyl chloride is shifted to higher temperatures. The amount of produced vinylchloride is higher at these temperatures than in presence of oxygen. CO and CO_2 are formed in lower amounts at higher temperatures. The shift of the vinyl chloride formation to higher temperatures is in agreement with the inhibition of the dehydrochlorination by water. At higher temperature less water will be adsorbed on the surface and therefore the inhibition will be decreased. The small amount of formed CO and CO_2 could be ascribed to the reaction of the formed vinylchloride with the surface oxygen of $LaMnO_{3+\delta}$.

In order to control this hypothesis, the catalyst was characterized by XRD before and after the reaction. No modification of the XRD and FTIR spectra could be observed with a catalyst working in presence of water and oxygen (Fig. 7a). After the reaction in presence of water without oxygen the structure of the catalyst is modified as can be seen in Fig. 7b. The features characteristic of a oxygen overstoichiometric

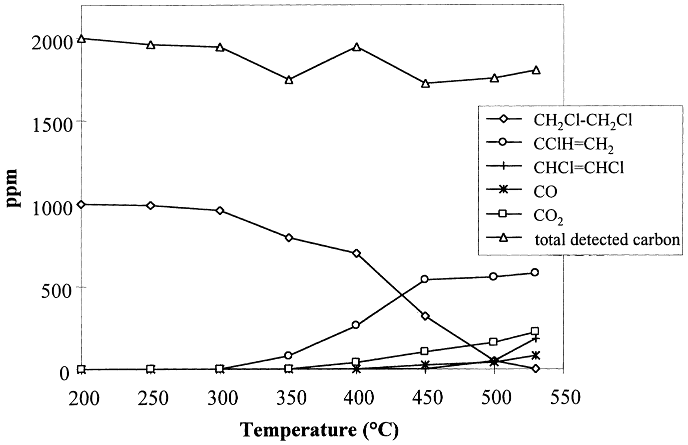

Fig. 6. Hydrolysis of 1000 ppm of $CH_2Cl–CH_2Cl$ on $LaMnO_{3+\delta}$ in He, without oxygen.

perovskite phase present in the fresh catalyst disappear and LaOCl, MnO and a small amount of stoichiometric $LaMnO_3$ are observed.

3.2. Catalyst ageing

It has previously been found [29] in the catalytic oxidation of dichloromethane and carbon tetrachloride in presence of water and oxygen that there is a difference of stability of $LaCoO_3$ and $LaMnO_{3+\delta}$. The $LaCoO_3$ structure is destroyed and LaOCl, and Co_3O_4 are formed. The cobalt particles sinter. The $LaMnO_{3+\delta}$ perovskite structure is not destroyed in these conditions as shown by FTIR, XRD and XPS. The difference in stability of the two perovskites was already suggested by the results during the preparation. Thus, $LaCoO_3$ could not be obtained from chloride precursors, whereas $LaMnO_{3+\delta}$ could be synthesized in the same conditions. XRD analyses have shown that the manganese containing structure (prepared by calcination in air) was overstoichiometric in oxygen. BET surface measurements before and after test show a decrease of the surface area of $LaMnO_{3+\delta}$ after reactivity with CCl_3CH_3, CH_2ClCH_2Cl and CCl_2CHCl from 17.1 $m^2\,g^{-1}$ to 11.7, 12.7 and 13.2 $m^2\,g^{-1}$, respectively.

The presence or the absence of the band perovskite characteristic at 604 cm^{-1} confirms the stability of $LaMnO_{3+\delta}$ in presence of oxygen and water and the destruction with water alone. The presence of MnO suggests that in absence of oxygen, the overstoichiometric $LaMnO_{3+\delta}$ perovskite is reduced. These results show that the stability of the manganese perovskite can probably be attributed to the oxygen overstoichiometry.

XPS measurements of $LaMnO_{3+\delta}$ and $LaCoO_3$ before and after reaction in presence of H_2O and O_2 and CCl_4 or CH_2Cl_2 confirm the stability of the $LaMnO_{3+\delta}$ structure. An example of the XPS $La3d_{5/2}$ spectrum is given in Fig. 8. The interpretation of the different spectra ($La3d_{5/2}$, $Mn2p_{1/2}$ and $2p_{3/2}$, Co $3p_{1/2}$ and $3p_{3/2}$) have been discussed in detail in [29] and the results are summarized on Table 3. For $La3d_{5/2}$, the peak at 833.7 eV has been attributed to La^{3+} of the perovskite. The signal at 835.7 eV to the La^{3+} of lanthanum surface carbonate. The peak at 837.8 eV and 839.0 eV are due to the strong screening effect of f electrons of the two first La^{3+} features. The $Mn2p_{1/2}$ (653.3 eV) and $Mn2p_{3/2}$ (641 eV) correspond to Mn^{3+}. The absence of a satellite at 5 eV from the main level excludes the presence of Mn^{2+}.

$Co2p_{1/2}$ (794.8 eV) and $Co2p_{3/2}$ (779 eV) cannot permit to distinguish between Co^{2+} and Co^{3+}, but the difference between these two levels is about 15.1 eV and points to Co^{3+}. For the used catalyst this difference if of 15.4 eV and indicates that some Co^{2+} (for which the difference is about 16 eV) may be present. Further a satellite at 789.9 eV suggest also the presence of some Co^{2+} but this peak is in general very intense and the amount of Co^{2+} on the surface is small. The Mn/La and Co/La ratios calculated from the XPS spectra are of 0.46 and 0.81 before reaction and 0.54

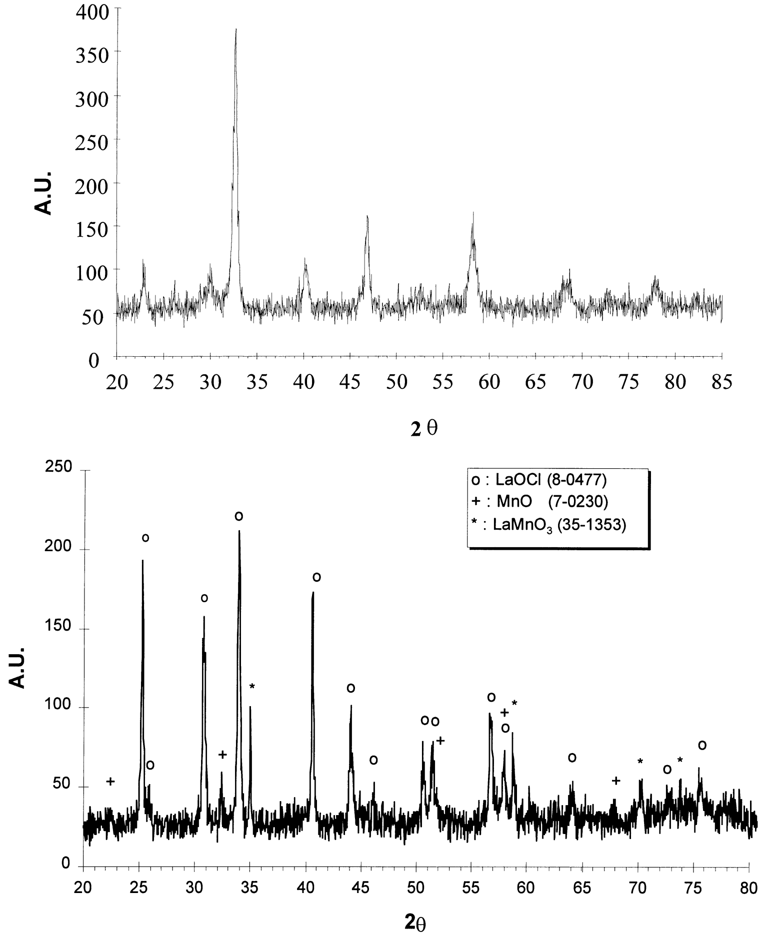

Fig. 7. (a) XRD spectrum of $LaMnO_{3+\delta}$ after reaction of 1000 ppm of $CH_2Cl–CH_2Cl$ in presence of 1.3% H_2O and 3.3% O_2 in He; (b) XRD spectrum of $LaMnO_{3+\delta}$ after reaction of 1000 ppm of $CH_2Cl–CH_2Cl$ in presence of 1.3% H_2O without O_2 in He.

(Mn/La) and 0.04 (Co/La) after reaction. These results indicate that the surface of $LaMnO_{3+\delta}$ is almost unchanged whereas Co is depleted from the surface of $LaCoO_3$. Given the depth of the XPS analysis one could conclude that Co migrates to the bulk. However results of SEM [29] show that $LaCoO_3$ is destroyed and big pyramidal particules of Co_3O_4 are formed. This is in agreement with the presence of some Co^{2+} on the surface and with the XRD spectra which show the formation of LaOCl and Co_3O_4 after reaction.

The stabilization enthalpy of the perovskite $\delta(LnMnO_3) = \Delta Gf°(LnMO_3) - 1/2\Delta Gf°(Ln_2O_3) - 1/2\ \Delta Gf°(M_2O_3)$ can be computed by the relation proposed by Yokokawa et al. [40].

The following results were obtained for $LaCoO_3$ and $LaMnO_3$: $\delta(LaCoO_3) = -36\ kJ\ mol^{-1}$ and $\delta(LaMnO_3) = -43.9\ kJ\ mol^{-1}$. It can be deduced that $LaCoO_3$ is slightly less stable than $LaMnO_3$.

In the reaction conditions, chlorine can be produced by the Deacon reaction, the following reactions must be taken into consideration, given the results from XRD.

$$LaCoO_3 + \tfrac{1}{2}Cl_2 \rightarrow LaOCl + \tfrac{1}{2}Co_3O_4 + \tfrac{1}{3}O_2 \qquad (R1)$$

$$LaMnO_3 + \tfrac{1}{2}Cl_2 \rightarrow LaOCl + MnO_2 \qquad (R2)$$

At higher temperatures CoO and MnO are the most stable oxide and the reactions to consider are

$$LaCoO_3 + \tfrac{1}{2}Cl_2 \rightarrow LaOCl + CoO + \tfrac{1}{2}O_2 \qquad (R3)$$

Table 3
Positions of the La3$d_{5/2}$, Mn2$p_{1/2}$, 2$p_{3/2}$, Co2$p_{1/2}$, and 2$p_{3/2}$. XPS peaks of $LaMnO_{3+\delta}$ and $LaCoO_3$ before and after reaction on CCl_4 and CH_2Cl_2

Catalysts	Peak position (eV); % of each peak			
	La3$d_{5/2}$			
$LaMnO_{3+\delta}$	833.9 (38.6)	335.7 (19.1)	837.8 (25.6)	839.0 (16.7)
$LaMnO_{3+\delta}$ after test CCl_4	833.7 (40.4)	835.5 (20.6)	837.7 (26.0)	838.9 (13.0)
$LaMnO_{3+\delta}$ after test CH_2Cl_2	833.5 (30.1)	835.3 (29.2)	837.6 (20.2)	838.7 (20.4)
$LaCoO_3$	833.5 (40.8)	835.7 (22.3)	837.8 (27.1)	839.1 (9.7)
$LaCoO_3$ after test CCl_4	833.8 (48.4)	835.6 (5.7)	837.9 (41.3)	839.0 (4.6)
$LaCoO_3$ after test CH_2Cl_2	834.0 (43.3)	835.8 (12.7)	838.1 (33.5)	839.0 (10.4)
	Mn2$p_{3/2}$	Mn2$p_{1/2}$		
$LaMnO_{3+\delta}$	641.7 (66.7)	653.3 (33.3		
$LaMnO_{3+\delta}$ after test CCl_4	641.7 (66.7)	653.0 (33.3)		
$LaMnO_{3+\delta}$ after test CH_2Cl_2	641.4 (66.7)	653.0 (33.3).		
	Co2$p_{3/2}$	Co2$p_{1/2}$	Satellite	
$LaCoO_3$	779.7 (65.4)	794.8 (32.6)	789.9 (2.0)	
$LaCoO_3$ After test CCl_4	779.0 (60.8)	794.4 (30.4)	789.8 (8.7	
$LaCoO_3$ After test CH_2Cl_2	779.1 (62.1)	794.5 (31.1)	790.5 (6.8)	

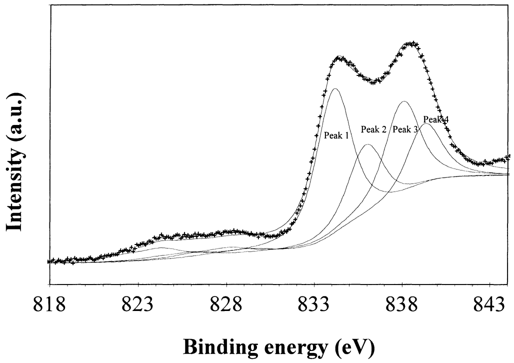

Fig. 8. Decomposition of the La3$d_{5/2}$ peak ($LaMnO_{3+\delta}$).

$$LaMnO_3 + \tfrac{1}{2}Cl_2 \rightarrow LaOCl + MnO + \tfrac{1}{2}O_2 \qquad (R4)$$

The free enthalpies of formation have been taken for the 'Handbook of Chemistry and Physics [41] or through Facility for Analysis of Chemical Thermodynamics (FACT) available on Internet [42]. The known free enthalpies of formation of $LaCoO_3$ and $LaMnO_3$ have been computed from the data of Yokokawa et al. [40] and the results obtained from FACT then compared to the experimental values. The fit was rather good and this validates the used data.

However, according to the results in XRD an oxygen overstoichiometric structure $LaMnO_{3+\delta}$ must be considered. Roosmalen et al. [43] have calculated the enthalpies and entropies for the overstoichiometric structure. Thus, the free enthalpies for the following reaction was also computed.

$$LaMnO_{3+\delta} + \tfrac{1}{2}Cl_2 \rightarrow LaOCl + MnO_2 + \tfrac{\delta}{2}O_2 \qquad (R5)$$

The obtained results are given in Fig. 9.

From these results it can be concluded that in presence of water and oxygen, the oxygen overstoichiometry can explain the stability of the manganese containing catalyst. In absence of oxygen in the feed, the framework oxygen takes part in the oxidation reaction, the manganese perovskite losing its oxygen overstoichiometry and its stability is destroyed according to reaction (R4) as shown by XRD of the used catalyst. FTIR experiments were made on adsorption of 1,2-dichloroethane on γ alumina [44] and the following scheme was proposed to explain the observed species (vinylchloride, acetaldehyde, acetate…).

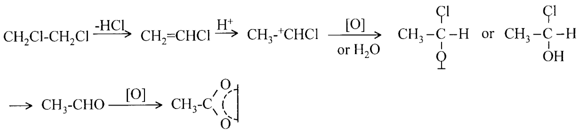

This scheme may also operate on the perovskites.

From our results it can be concluded that for 1,2-dichloroethane destruction on perovskite both water and oxygen are necessary. Water prevents polymerization on the surface or the exit of the reactor

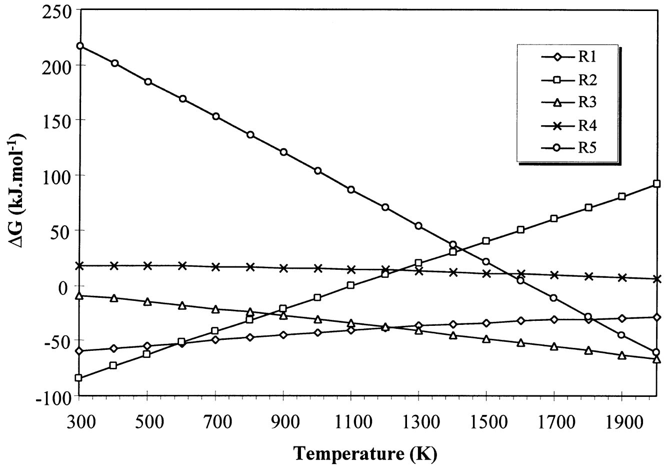

Fig. 9. Free enthalpy for chlorination reaction with $LaMnO_3$ and $LaCoO_3$.

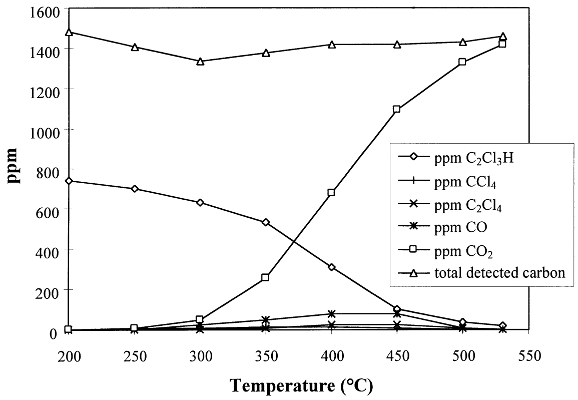

Fig. 10. Oxidation of 750 ppm of $CCl_2=CHCl$ on 0.5 g of $LaMnO_{3+\delta}$ in presence of 3.3% O_2, 1.3% H_2O in He.

and oxygen is necessary to prevent the reduction of the perovskite, maintaining in the case of $LaMnO_{3+\delta}$, the oxygen overstoichiometry and avoiding such destruction of the perovskite structure.

Trichloroethylene was chosen as a model for unsaturated chlorinated C_2 hydrocarbons, since it is also known that on Pt/Al_2O_3 catalysts, it is difficult to destroy. Windawi and Wyatt [6] have found 90% conversion at 500°C. Oxidation of trichloroethylene in the presence of water and oxygen is represented in Fig. 10. A T_{50} value of 360°C and a T_{90} value of 500°C are obtained in our conditions.

The influence of water was also studied as can be seen in Fig. 11.

Water has a beneficial effect on both conversion and CO_x formation. This effect is higher for trichloroethylene than for 1,2-dichloroethane. The observed difference could be explained by assuming that vinylchloride is an intermediate in 1,2-dichloroethane oxidation. Water inhibits the dehydrochlorination reaction and therefore decreases slightly the rate of 1,2-dichloroethane conversion. With trichloroethylene only the beneficial effect of water on the oxidation is observed.

Finally, the aromatic chlorinated compounds are modelized by chlorobenzene and the conversion is represented in Fig. 12. A T_{50} value of 420°C is obtained and chlorobenzene is almost completely destroyed at 500°C.

Influence of water is given in Fig. 13. Both conversion and CO_x formation are almost not affected by the presence of water. The conversion and CO_x formation curves are very near to each other showing thus that only traces amounts of by-products are formed.

The low effect of water, on the conversion of chlorobenzene might be attributed to its low Cl/H ratio. If the following scheme is taken water is formed during the reaction

$$ClC_6H_5 \rightarrow CO_2 + 2H_2O + HCl$$

Since 1000 ppm of chlorobenzene are introduced 2000 ppm of water is produced at total conversion. The analysis of polychlorinated compounds show that in presence of water only ppm amounts of higher

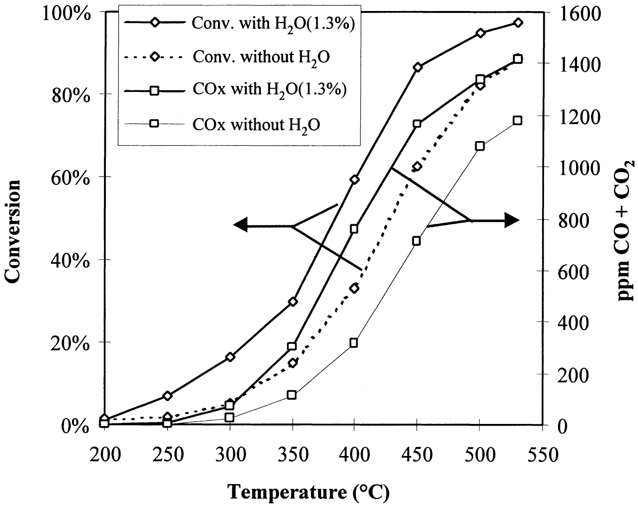

Fig. 11. Influence of water or conversion of trichloroethylene and CO_x formation on $LaMnO_{3+\delta}$ in presence of 3.3% O_2 in He.

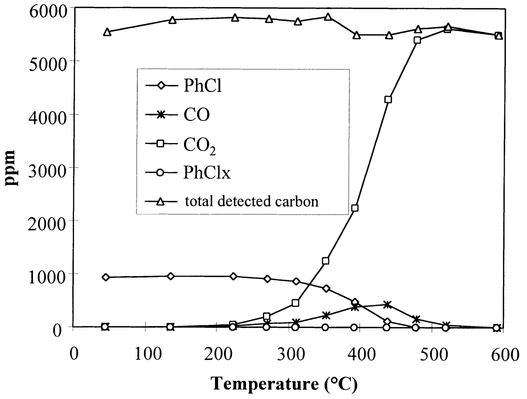

Fig. 12. Destruction of chlorobenzene on $LaMnO_{3+\delta}$ in presence of 1% H_2O, 15% O_2 in He.

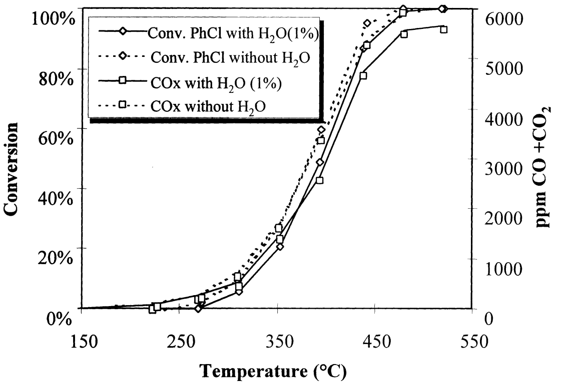

Fig. 13. Influence of water on the conversion of 1000 ppm of chlorobenzene on $LaMnO_{3+\delta}$ in presence of 15% O_2 in He.

chlorinated compounds are formed. Water has thus a beneficial effect on the selectivity of the perovskite to CO_2 and HCl. This can be attributed to the reverse Deacon reaction in presence of additional water, decreasing the formation of Cl_2 and hence preventing chlorination of chlorobenzene.

4. Conclusion

Perovskites have shown to be active in catalytic oxidation of chlorinated volatile organic compounds, may it be chloromethanes, C_2 chlorinated hydrocarbons or aromatics. $LaCoO_3$ and $LaMnO_{3+\delta}$ have shown to be the most active ones in term of activity per weight of catalyst. A difference in stability was however observed for these two perovskite structures. The analysis of the used catalysts by various techniques like FTIR, XRD and XPS have shown that this difference can be ascribed to the destruction of the cobalt containing perovskites and formation of LaOCl and Co_3O_4. The results obtained in the oxidation of 1,2-dichloroethane in absence of oxygen have shown that the manganese containing perovskite was destroyed suggesting that reduction is the cause of the diminution of the stability. Thermodynamic consideration suggest that the higher resistance of $LaMnO_{3+\delta}$ can be attributed to its oxygen overstoichiometry.

Despite their promising properties perovskites have still some drawbacks like their low specific surface area. The results obtained in the present work show that it is worthy to continue to work on well defined mixed oxide structures. The resistance of the oxygen overstoichiometric manganese perovskite suggests that other mixed oxide structures which can accommodate oxygen overstoichiometry should be considered.

Acknowledgements

The authors are indebted to ADEME, to Region Alsace (France) and E.C. (contract EV5V-CT94-0530) for their financial support. Further they should like to thank R. van den Brink (Leiden-Netherlands) for the analyses of polychlorinated aromatic compounds in the reaction of chlorobenzene.

References

[1] H. Sidebottom, J. Franklin, Pure Appl. Chem. 68(9) (1996) 1757.
[2] E. Nordally, J.R. Richmond, K.J. Drumm, in: S. Vineron, J. Chaouki (Eds.), Stud. Environ. Sci., Elsevier, Amsterdam, vol. 61, 1994, p. 459.
[3] J.J. Spivey, Ind. Eng. Chem. Res. 26 (1987) 2165.
[4] A. Schwartz, L. Holbrook, H. Wise, J. Catal. 21 (1971) 199.
[5] H. Windawi, Z.C. Zhang, Catal. Today 30 (1996) 99.
[6] H. Windawi, M. Wyatt, Plat. Met. Rev. 37 (1993) 186.
[7] D.M. Papenmeier, J.A. Rossin, Ind. Eng. Chem. Res. 33 (1994) 3094.
[8] J.A. Rossin, M.M. Farnis, Ind. Eng. Chem. Res. 32 (1993) 1024.
[9] H. Shaw, Y. Wang, A.E. Cerkanowicz, A.C.S. Symp. Series 518 (1993) 358.
[10] H. Müller, K. Deller, B. Despeyroux, E. Peldszus, Catal. Today 17 (1993) 383.
[11] T.M. Friedel, A.C. Frost, K.J. Herbert, F. Meyer, J.C. Summers, Catal. Today 17 (1993) 367.
[12] J.J. Spivey, J.B. Butt, Catal. Today 11 (1992) 547.
[13] K. Yang, J.B. Reedy, US Patent 4,05,9676 (1977).
[14] A.T. Dalton, S. Sircar, US Patent 4,346,019 (1982).
[15] S.C. Petrosius, R.S. Drago, V. Young, G.C. Grunenwald, J. Am. Chem. Soc. 115 (1993) 6131.
[16] F. Solymosi, J. Rasko, E. Papp, A. Oszoko, T. Bansagi, Applied Catal. A. Gen. 131 (1995) 55.
[17] L. Stoaro, R. Ganzerla, M. Lenarda, R. Zanoni, A.J. Lopez, P. Olivera-Pastor, E. Castellon, J. Mol. Catal. A. Chem. 115 (1997) 329.
[18] K. Griesbaum, D. Hönicke, A. Haas, F. Schwerdtner, 213th Nat. Meeting A.C.S. San Francisco, 13–17 April 1997, p. 175.
[19] P. Manning, Hazard Waste 1 (1984) 41.
[20] R. Michalowicz, The oxidation of chlorinated ethylenes using selected catalysts, M.S. Thesis, MIT Press, Cambridge. MA, September 1982, from reference 12.
[21] S.K. Agarwal, J.J. Spivey, J.B. Butt, Applied Catal. A. Gen. 82 (1992) 259.
[22] T. Seiyama, Properties and Applications of Perovskite Type Oxides, in: L.G. Tejuca, J.L.G. Fiero (Eds.), Marcel Dekker, New York, 1993, p. 215.
[23] G. Sinquin, S. Libs, I. Gassiot, C. Petit, J.P. Hindermann, A. Kiennemann, Odours VOC's Journal 1 (1995) 157.
[24] R. Schneider, D. Kiessling, P. Kraak, M. Haftendorn, G. Wendt, Chem. Tech. 47 (1995) 199.
[25] G. Sinquin, S. Libs, C. Petit, J.P. Hindermann, A. Kiennemann, 11th Int. Congr. Catal., 40th Anniversary Baltimore, 30 June to 5 July 1996, poster 264.
[26] G. Wendt, M. Hackenberger, D. Kiessling, R. Schneider, P. Kraak, 11th Int. Congr. Catal., 40th Anniversary Baltimore, 30 June to 5 July 1996, poster 274.
[27] C. Petit, A. Kaddouri, S. Libs, A. Kiennemann, J.L. Rehspringer, P. Poix, J. Catal. 140 (1993) 328.
[28] A.C. Roger, C. Petit, A. Kiennemann, J. Catal. 167 (1997) 447.
[29] G. Sinquin, C. Petit, J.P. Hindermann, A. Kiennemann, Chemistry Energy and the Environment. The Royal Society of Chemistry (C.A.C. Sequeira, J.B. Moftat, Eds.).
[30] M. Romeo, J. Majerus, P. Legaré, N.J. Castellani, D.B. Leroy, Surf. Sci. 238 (1990) 163.
[31] M. Romeo, K. Bak, J. El-Fallah, F. Le Normand, L. Hilaire, Surf. Interface Anal. 20 (1993) 508.
[32] G. Sinquin, C. Petit, S. Libs, J.P. Hindermann, A. Kiennemann, Appl. Catal. B, submitted for publication.
[33] J.F. Haw, T. Xu, J.B. Nicholas, P.W. Goguen, Nature 389 (1997) 832.
[34] R. van den Brink, P. Mulder, R. Louw, G. Sinquin, C. Petit, J.P. Hindermann, J. Catal. 180 (1998) 153.
[35] T. Mochida, A. Uchimo, H. Fujitsu, K. Takeshita, J. Catal. 32 (1967) 3894.
[36] A.E. Kulikova, E.N. Zil'berman, Russian Chem. Rev. 67 (1991) 127.
[37] T.H. Ballinger, J.T. Yates Jr., J. Phys. Chem. 96 (1992) 1417.
[38] E.E. Getty, S.C. Petrosius, R.S. Drago, J. Mol. Catal. 67 (1991) 127.
[39] S.I. Imamura, H. Tarumoto, S. Ishida, Ind. Eng. Chem. Res. 28 (1989) 1449.
[40] H. Yokokawa, N. Sakai, K. Dokiya, M. Dokiya, Solid State Ionics 52 (1992) 43.
[41] Handbook of Chemistry and Physics, 6th ed., 1983–1984, CRC Press, Boca Raton, Florida.
[42] F.A.C.T. Programm http://www:crct.polymtl.ca/FACT/fact.htw.
[43] J.A.M. Roosmalen, E.H.P. Cordfunke, J. Solid State Chem. 110 (1994) 109.
[44] M.M.R. Feijen-Jeurissen, J.J. Jorna, B.E. Nieuwenhuys, G. Sinquin, J.P. Hindermann, C. Petit, Catal. Today, this issue.